

Theory of magnons in spin systems with Dzyaloshinskii-Moriya interaction

Sahbi El Hog and H. T. Diep
*Laboratoire de Physique Théorique et Modélisation,
Université de Cergy-Pontoise, CNRS, UMR 8089
2, Avenue Adolphe Chauvin,
95302 Cergy-Pontoise Cedex, France.*

Henryk Puzzkarski
*Surface Physics Division, Faculty of Physics,
Adam Mickiewicz University,
ul. Umultowska 85, 61-614 Poznan, Poland.*
(Dated: June 10, 2021)

We study in this paper magnetic properties of a system of quantum Heisenberg spins interacting with each other via a ferromagnetic exchange interaction J and an in-plane Dzyaloshinskii-Moriya interaction D . The non-collinear ground state due to the competition between J and D is determined. We employ a self-consistent Green's function theory to calculate the spin-wave spectrum and the layer magnetizations at finite T in two and three dimensions as well as in a thin film with surface effects. Analytical details and the validity of the method are shown and discussed.

PACS numbers: 75.25.-j ; 75.30.Ds ; 75.70.-i :

I. INTRODUCTION

The Dzyaloshinskii-Moriya (DM) interaction was proposed to explain the weak ferromagnetism which was observed in antiferromagnetic Mn compounds. The phenomenological Landau-Ginzburg model introduced by I. Dzyaloshinskii [1] was microscopically derived by T. Moriya [2]. The interaction between two spins \mathbf{S}_i and \mathbf{S}_j is written as

$$\mathbf{D}_{i,j} \cdot \mathbf{S}_i \wedge \mathbf{S}_j \quad (1)$$

where $\mathbf{D}_{i,j}$ is a vector which results from the displacement of non magnetic ions located between \mathbf{S}_i and \mathbf{S}_j , for example in Mn-O-Mn bonds. The direction of $\mathbf{D}_{i,j}$ depends on the symmetry of the displacement [2]. The DM interaction is antisymmetric with respect to the inversion symmetry.

There has been a large number of investigations on the effect of the DM interaction in various materials, both experimentally and theoretically for weak ferromagnetism in perovskite compounds (see references cited in Refs. 3 and 4, for example). However, the interest in the DM interaction goes beyond the weak ferromagnetism: for example, it has been recently shown in various works that the DM interaction is at the origin of topological skyrmions [5–16] and new kinds of magnetic domain walls [17, 18]. The increasing interest in skyrmions results from the fact that skyrmions may play an important role in the electronic transport which is at the heart of technological application devices [19].

In this paper, we are interested in the spin-wave (SW) properties of a system of spins interacting with each other via a DM interaction in addition to the symmet-

ric isotropic Heisenberg exchange interaction. The competition between these interactions gives rise to a non-collinear spin configuration in the ground state (GS). Unlike helimagnets where the helical GS spin configuration results from the competition between the symmetric nearest-neighbor (NN) and next-nearest neighbor (NNN) interactions [20, 21], the DM interaction, as said above, is antisymmetric. This gives rise to a non trivial SW behavior as will be seen below. Note that there has been a number of works dealing with the SW properties in DM systems [22–26].

This paper is organized as follows. Section II is devoted to the description of the model and the determination of the GS. Section III shows the formulation of our self-consistent Green's function (GF) method. Section IV shows results on the SW spectrum and the magnetization in two dimensions (2D) and three dimensions (3D). The case of thin films with free surfaces is shown in section V where layer magnetizations at finite temperature (T) and the thickness effect are presented. Concluding remarks are given in section VI.

II. MODEL AND GROUND STATE

We consider a thin film of simple cubic (SC) lattice of N layers stacked in the y direction perpendicular to the film surface. For the reason which is shown below, we choose the film surface as a xz plane. The Hamiltonian is given by

$$\mathcal{H} = \mathcal{H}_e + \mathcal{H}_{DM} \quad (2)$$

$$\mathcal{H}_e = - \sum_{\langle i,j \rangle} J_{i,j} \mathbf{S}_i \cdot \mathbf{S}_j \quad (3)$$

$$\mathcal{H}_{DM} = \sum_{\langle i,j \rangle} \mathbf{D}_{i,j} \cdot \mathbf{S}_i \wedge \mathbf{S}_j \quad (4)$$

where $J_{i,j}$ and $\mathbf{D}_{i,j}$ are the exchange and DM interactions, respectively, between two Heisenberg spins \mathbf{S}_i and \mathbf{S}_j of magnitude $S = 1/2$ occupying the lattice sites i and j .

For simplicity, let us consider the case where the in-plane and inter-plane exchange interactions between NN are both ferromagnetic and denoted by J_{\parallel} and J_{\perp} , respectively. The DM interaction is supposed to be between NN in the plane with a constant D . Due to the competition between the exchange J term which favors the collinear configuration, and the DM term which favors the perpendicular one, we expect that the spin \mathbf{S}_i makes an angle $\theta_{i,j}$ with its neighbor \mathbf{S}_j . Therefore, the quantization axis of \mathbf{S}_i is not the same as that of \mathbf{S}_j . Let us call $\hat{\xi}_i$ the quantization axis of \mathbf{S}_i and $\hat{\xi}_i^{\perp}$ its perpendicular axis in the xz plane. The third axis $\hat{\eta}_i$, perpendicular to the film surface, is chosen in such a way to make $(\hat{\xi}_i, \hat{\eta}_i, \hat{\xi}_i^{\perp})$ an orthogonal direct frame. Writing \mathbf{S}_i and \mathbf{S}_j in their respective local coordinates, one has

$$\mathbf{S}_i = S_i^x \hat{\xi}_i + S_i^y \hat{\eta}_i + S_i^z \hat{\xi}_i^{\perp} \quad (5)$$

$$\mathbf{S}_j = S_j^x \hat{\xi}_j + S_j^y \hat{\eta}_j + S_j^z \hat{\xi}_j^{\perp} \quad (6)$$

We choose the vector $\mathbf{D}_{i,j}$ perpendicular to the xz plane, namely

$$\mathbf{D}_{i,j} = D e_{i,j} \hat{\eta}_i \quad (7)$$

where $e_{i,j} = +1$ (-1) if $j > i$ ($j < i$) for NN on the $\hat{\xi}_i$ or $\hat{\xi}_i^{\perp}$ axis. Note that $e_{j,i} = -e_{i,j}$.

To determine the GS, the easiest way is to use the steepest descent method: we calculate the local field acting on each spin from its neighbors and we align the spin in its local-field direction to minimize its energy. Repeating this for all spins and iterating many times until the convergence is reached with a desired precision (usually at the 6-th digit, namely at $\simeq 10^{-6}$ per cents), we obtain the lowest energy state of the system (see Ref. 27). Note that we have used several thousands of different initial conditions to check the convergence to a single GS for each set of parameters. Choosing $\mathbf{D}_{i,j}$ lying perpendicular to the spin plane (i. e. xz plane) as indicated in Eq. (7), we determine the GS as a function of D . An example is shown in Fig. 1 for $\theta = \pi/6$ ($D = -0.577$) with $J_{\parallel} = J_{\perp} = 1$. We see that each spin has the same angle with its four NN in the plane (angle between NN in adjacent planes is zero). Let us show the relation between θ and J_{\parallel} : the energy of the spin \mathbf{S}_i is written as

$$E_i = -4J_{\parallel} S^2 \cos \theta - 2J_{\perp} S^2 + 4DS^2 \sin \theta \quad (8)$$

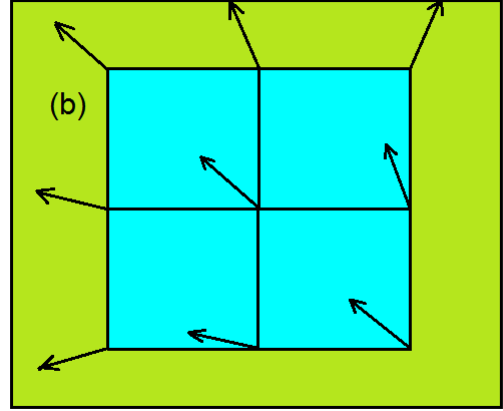
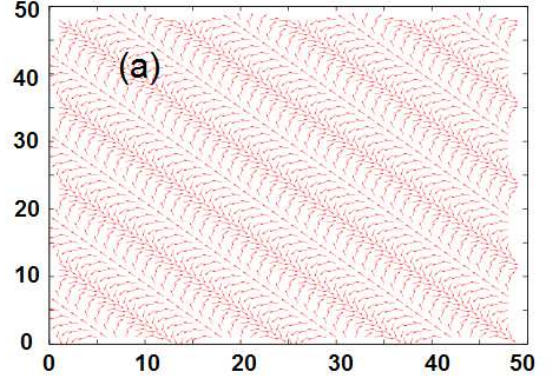


FIG. 1. (a) The ground state is a planar configuration on the xz plane. The figure shows the case where $\theta = \pi/6$ ($D = -0.577$), $J_{\parallel} = J_{\perp} = 1$ using the steepest descent method ; (b) a zoom is shown around a spin with its nearest neighbors.

where $\theta = |\theta_{i,j}|$ and care has been taken on the signs of $\sin \theta_{i,j}$ and $e_{i,j}$ when counting NN, namely two opposite NN have opposite signs. The minimization of E_i yields

$$\frac{dE_i}{d\theta} = 0 \Rightarrow -\frac{D}{J_{\parallel}} = \tan \theta \Rightarrow \theta = \arctan\left(-\frac{D}{J_{\parallel}}\right) \quad (9)$$

The value of θ for a given $\frac{D}{J_{\parallel}}$ is precisely what obtained by the steepest descent method.

In the present model, the DM interaction is supposed in the plane, so in the GS the angle between in-plane NN is not zero. We show in Fig. 1 the relative orientation of the two NN spins in the plane.

Note that the perpendicular axes $\hat{\eta}_i$ and $\hat{\eta}_j$ coincide. Now, expressing the local frame of \mathbf{S}_j in the local frame of \mathbf{S}_i , we have

$$\hat{\xi}_j = \cos \theta_{i,j} \hat{\xi}_i + \sin \theta_{i,j} \hat{\xi}_i^{\perp} \quad (10)$$

$$\hat{\xi}_j^{\perp} = -\sin \theta_{i,j} \hat{\xi}_i + \cos \theta_{i,j} \hat{\xi}_i^{\perp} \quad (11)$$

$$\hat{\eta}_j = \hat{\eta}_i \quad (12)$$

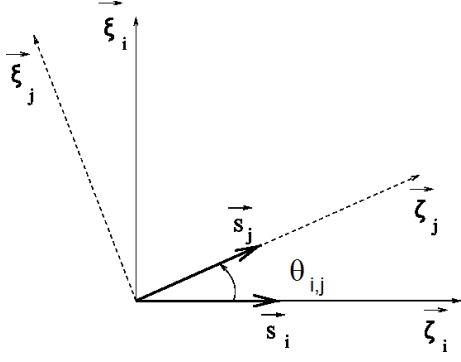


FIG. 2. Local coordinates in the xz plane. The spin quantization axes of \mathbf{S}_i and \mathbf{S}_j are $\hat{\zeta}_i$ and $\hat{\zeta}_j$, respectively.

so that

$$\begin{aligned} \mathbf{S}_j = & S_j^x (\cos \theta_{i,j} \hat{\zeta}_i - \sin \theta_{i,j} \hat{\xi}_i) \\ & + S_j^y \hat{\eta}_i + S_j^z (\cos \theta_{i,j} \hat{\zeta}_i + \sin \theta_{i,j} \hat{\xi}_i) \end{aligned} \quad (13)$$

The DM term of Eq. (4) can be rewritten as

$$\begin{aligned} \mathbf{S}_i \wedge \mathbf{S}_j = & (-S_i^z S_j^y - S_i^y S_j^x \sin \theta_{i,j} + S_i^y S_j^z \cos \theta_{i,j}) \hat{\xi}_i \\ & + (S_i^x S_j^x \sin \theta_{i,j} + S_i^z S_j^z \sin \theta_{i,j}) \hat{\eta}_i \\ & + (S_i^y S_j^y - S_i^x S_j^z \sin \theta_{i,j} - S_i^z S_j^x \cos \theta_{i,j}) \hat{\zeta}_i \end{aligned} \quad (14)$$

Using Eq. (7), we have

$$\begin{aligned} \mathcal{H}_{DM} = & \sum_{\langle i,j \rangle} \mathbf{D}_{i,j} \cdot \mathbf{S}_i \wedge \mathbf{S}_j \\ = & D \sum_{\langle i,j \rangle} (S_i^x S_j^x e_{i,j} \sin \theta_{i,j} + S_i^z S_j^z e_{i,j} \sin \theta_{i,j}) \\ = & \frac{D}{4} \sum_{\langle i,j \rangle} [(S_i^+ + S_i^-)(S_j^+ + S_j^-) e_{i,j} \sin \theta_{i,j} \\ & + 4S_i^z S_j^z e_{i,j} \sin \theta_{i,j}] \end{aligned} \quad (15)$$

where we have replaced $S^x = (S^+ + S^-)/2$. Note that $e_{i,j} \sin \theta_{i,j}$ is always positive since for a NN on the positive axis direction, $e_{i,j} = 1$ and $\sin \theta_{i,j} = \sin \theta$ where θ is positively defined, while for a NN on the negative axis direction, $e_{i,j} = -1$ and $\sin \theta_{i,j} = \sin(-\theta) = -\sin \theta$.

Note that for non collinear spin configurations, the local spin coordinates allow one to use the commutation relations between spin operators of a spin which are valid only when the z spin component is defined on its quantification axis. This method has been applied for helimagnets [28–30].

III. SELF-CONSISTENT GREEN'S FUNCTION METHOD: FORMULATION

The GF method has been developed for non collinear surface spin configurations in thin films [27, 31–33]. Let

us briefly recall here the principal steps of calculation and give the results for the present model. Expressing the Hamiltonian in the local coordinates, we obtain

$$\begin{aligned} \mathcal{H} = & - \sum_{\langle i,j \rangle} J_{i,j} \left\{ \frac{1}{4} (\cos \theta_{i,j} - 1) (S_i^+ S_j^+ + S_i^- S_j^-) \right. \\ & + \frac{1}{4} (\cos \theta_{i,j} + 1) (S_i^+ S_j^- + S_i^- S_j^+) \\ & + \frac{1}{2} \sin \theta_{i,j} (S_i^+ + S_i^-) S_j^z - \frac{1}{2} \sin \theta_{i,j} S_i^z (S_j^+ + S_j^-) \\ & \left. + \cos \theta_{i,j} S_i^z S_j^z \right\} \\ & + \frac{D}{4} \sum_{\langle i,j \rangle} [(S_i^+ + S_i^-)(S_j^+ + S_j^-) e_{i,j} \sin \theta_{i,j} \\ & + 4S_i^z S_j^z e_{i,j} \sin \theta_{i,j}] \end{aligned} \quad (16)$$

As said in the previous section, the spins lie in the xz planes, each on its quantization local z axis (Fig. 2).

Note that unlike the sinus term of the DM Hamiltonian, Eq. (15), the sinus terms of \mathcal{H}_e , the 3rd line of Eq. (16), are zero when summed up on opposite NN (no $e_{i,j}$ to compensate). The 3rd line disappears therefore in the following.

At this stage it is very important to note that the standard commutation relations between spin operators S^z and S^\pm are defined with z as the spin quantization axis. In non collinear spin configurations, calculations of SW spectrum using commutation relations without paying attention to this are wrong.

It is known that in two dimensions (2D) there is no long-range order at finite temperature (T) for isotropic spin models with short-range interaction [34]. Thin films have small thickness, therefore to stabilize the ordering at finite T it is useful to add an anisotropic interaction. We use the following anisotropy between \mathbf{S}_i and \mathbf{S}_j which stabilizes the angle determined above between their local quantization axes S_i^z and S_j^z :

$$\mathcal{H}_a = - \sum_{\langle i,j \rangle} I_{i,j} S_i^z S_j^z \cos \theta_{i,j} \quad (17)$$

where $I_{i,j}$ is supposed to be positive, small compared to $J_{i,j}$, and limited to NN. Hereafter we take $I_{i,j} = I_1$ for NN pair in the xz plane, for simplicity. As it turns out, this anisotropy helps stabilize the ordering at finite T in 2D as discussed. It helps also stabilize the SW spectrum at $T = 0$ in the case of thin films but it is not necessary for 2D and 3D at $T = 0$. The total Hamiltonian is finally given by

$$\mathcal{H} = \mathcal{H}_e + \mathcal{H}_{DM} + \mathcal{H}_a \quad (18)$$

We define the following two double-time GF's in the

real space

$$G_{i,j}(t, t') = \langle\langle S_i^+(t); S_j^-(t') \rangle\rangle \\ = -i\theta(t - t') \langle [S_i^+(t), S_j^-(t')] \rangle \quad (19)$$

$$F_{i,j}(t, t') = \langle\langle S_i^-(t); S_j^-(t') \rangle\rangle \\ = -i\theta(t - t') \langle [S_i^-(t), S_j^-(t')] \rangle \quad (20)$$

The equations of motion of these functions read

$$i\hbar \frac{dG_{i,j}(t, t')}{dt} = \langle [S_i^+(t), S_j^-(t')] \rangle \delta(t - t') \\ - \langle\langle [\mathcal{H}, S_i^+]; S_j^- \rangle\rangle \quad (21)$$

$$i\hbar \frac{dF_{i,j}(t, t')}{dt} = \langle [S_i^-(t), S_j^-(t')] \rangle \delta(t - t') \\ - \langle\langle [\mathcal{H}, S_i^-]; S_j^- \rangle\rangle \quad (22)$$

For the \mathcal{H}_e and \mathcal{H}_a parts, the above equations of motion generate terms such as $\langle\langle S_i^z S_i^\pm; S_j^\pm \rangle\rangle$ and $\langle\langle S_i^\pm S_i^\pm; S_j^\pm \rangle\rangle$. These functions can be approximated by using the Tyablikov decoupling to reduce to the above-defined G and F functions:

$$\langle\langle S_i^z S_i^\pm; S_j^\pm \rangle\rangle \simeq \langle S_i^z \rangle \langle\langle S_i^\pm; S_j^\pm \rangle\rangle \quad (23) \\ \langle\langle S_i^\pm S_i^\pm; S_j^\pm \rangle\rangle \simeq \langle S_i^\pm \rangle \langle\langle S_i^\pm; S_j^\pm \rangle\rangle \simeq 0 \quad (24)$$

The last expression is due to the fact that transverse SW motions $\langle S_i^\pm \rangle$ are zero with time. For the DM term, the commutation relations $[\mathcal{H}, S_i^\pm]$ give rise to the following term:

$$D \sum_l \sin \theta [\mp S_i^z (S_l^+ + S_l^-) \pm 2S_i^\pm S_l^z] \quad (25)$$

which leads to the following type of GF's:

$$\langle\langle S_i^z S_l^\pm; S_j^\pm \rangle\rangle \simeq \langle S_i^z \rangle \langle\langle S_l^\pm; S_j^\pm \rangle\rangle \quad (26)$$

Note that we have replaced $e_{i,j} \sin \theta_{i,j}$ by $\sin \theta$ where θ is positive. The above equation is related to G and F functions [see Eq. (24)]. The Tyablikov decoupling scheme neglects higher-order functions.

We now introduce the following in-plane Fourier transforms $g_{n,n'}$ and $f_{n,n'}$ of the G and F Green's functions:

$$G_{i,j}(t, t', \omega) = \frac{1}{\Delta} \int_{BZ} d\vec{k}_{xz} e^{-i\omega(t-t')} \\ \times g_{n,n'}(\omega, \vec{k}_{xz}) e^{i\vec{k}_{xz} \cdot (\vec{R}_i - \vec{R}_j)} \quad (27)$$

$$F_{i,j}(t, t', \omega) = \frac{1}{\Delta} \int_{BZ} d\vec{k}_{xz} e^{-i\omega(t-t')} \\ \times f_{n,n'}(\omega, \vec{k}_{xz}) e^{i\vec{k}_{xz} \cdot (\vec{R}_i - \vec{R}_j)} \quad (28)$$

where the integral is performed in the first xz Brillouin zone (BZ) of surface Δ , ω is the spin-wave frequency, n and n' are the indices of the layers along the c axis to which \vec{R}_i and \vec{R}_j belong ($n = 1$ being the surface layer, $n = 2$ the second layer and so on). We finally obtain the following matrix equation

$$\mathbf{M}(E) \mathbf{h} = \mathbf{u}, \quad (29)$$

where $\mathbf{M}(E)$ is a square matrix of dimension $(2N \times 2N)$, \mathbf{h} and \mathbf{u} are the column matrices which are defined as follows

$$\mathbf{h} = \begin{pmatrix} g_{1,n'} \\ f_{1,n'} \\ \vdots \\ g_{n,n'} \\ f_{n,n'} \\ \vdots \\ g_{N,n'} \\ f_{N,n'} \end{pmatrix}, \quad \mathbf{u} = \begin{pmatrix} 2 \langle S_1^z \rangle \delta_{1,n'} \\ 0 \\ \vdots \\ 2 \langle S_N^z \rangle \delta_{N,n'} \\ 0 \end{pmatrix}, \quad (30)$$

where $E = \hbar\omega$ and $\mathbf{M}(E)$ is given by

$$\begin{pmatrix} E + A_1 & B_1 & C_1 & 0 & 0 & 0 & 0 & 0 & 0 \\ -B_1 & E - A_1 & 0 & -C_1 & 0 & 0 & 0 & 0 & 0 \\ \dots & \dots & \dots & \dots & \dots & \dots & \dots & \dots & \dots \\ \dots & 0 & C_n & 0 & E + A_n & B_n & C_n & 0 & 0 \\ \dots & 0 & 0 & -C_n & -B_n & E - A_n & 0 & -C_n & 0 \\ \dots & \dots & \dots & \dots & \dots & \dots & \dots & \dots & \dots \\ 0 & 0 & 0 & 0 & 0 & C_N & 0 & E + A_N & B_N \\ 0 & 0 & 0 & 0 & 0 & 0 & -C_N & -B_N & E - A_N \end{pmatrix} \quad (31)$$

with

$$A_n = -J_{\parallel} [8 \langle S_n^z \rangle \cos \theta (1 + d_n) \\ -4 \langle S_n^z \rangle \gamma (\cos \theta + 1)] \\ -2J_{\perp} (\langle S_{n-1}^z \rangle + \langle S_{n+1}^z \rangle) \\ -4D \sin \theta \langle S_n^z \rangle \gamma \\ +8D \sin \theta \langle S_n^z \rangle \quad (32)$$

$$B_n = 4J_{\parallel} \langle S_n^z \rangle \gamma (\cos \theta - 1) \\ -4D \sin \theta \langle S_n^z \rangle \gamma \quad (33)$$

where $n = 1, 2, \dots, N$, $d_n = I_1/J_{\parallel}$, $\gamma = (\cos k_x a + \cos k_z a)/2$, k_x and k_z denote the wave-vector components in the xz planes, a the lattice constant. Note that (i) if

$n = 1$ (surface layer) then there are no $n - 1$ terms in the matrix coefficients, (ii) if $n = N$ then there are no $n + 1$ terms. Besides, we have distinguished the in-plane NN interaction J_{\parallel} from the inter-plane NN one J_{\perp} .

In the case of a thin film, the SW eigenvalues at a given wave vector $\vec{k} = (k_x, k_z)$ are calculated by diagonalizing the matrix .

The layer magnetization of the layer n is given by (see technical details in Ref. 36):

$$\langle S_n^z \rangle = \frac{1}{2} - \frac{1}{\Delta} \int \int dk_x dk_z \sum_{i=1}^{2N} \frac{Q_{2n-1}(E_i)}{e^{E_i/k_B T} - 1} \quad (35)$$

where $n = 1, \dots, N$, and $Q_{2n-1}(E_i)$ is the determinant obtained by replacing the $(2n - 1)$ -th column of \mathbf{M} by \mathbf{u} at E_i .

The layer magnetizations can be calculated at finite temperatures self-consistently using the above formula. The numerical method to carry out this task has been described in details in Refs. 32. One can summarize here: (i) using a set of trial values (inputs) for $\langle S_n^z \rangle$ ($n = 1, \dots, N$), one diagonalizes the matrix to find spin-wave energies E_i which are used to calculate the outputs $\langle S_n^z \rangle$ ($n = 1, \dots, N$) by using Eq. (35), (ii) using the outputs as inputs to iterate the equations, (iii) if the output values are the same as the inputs within a precision (usually at 0.001%), the iteration is stopped. The method is thus self-consistent.

The value of the spin in the layer n at $T = 0$ is calculated by [32, 36]

$$\langle S_n^z \rangle(T = 0) = \frac{1}{2} + \frac{1}{\Delta} \int \int dk_x dk_z \sum_{i=1}^N Q_{2n-1}(E_i) \quad (36)$$

where the sum is performed over N negative values of E_i (for positive values, the Bose-Einstein factor in Eq. (35) is equal to 0 at $T = 0$).

The transition temperature T_c can be calculated by letting $\langle S_n^z \rangle$ on the left-hand side of Eq. (35) to go to zero. The energy E_i tends then to zero, so that we can make an expansion of the exponential at $T = T_c$. We have

$$\left[\frac{1}{k_B T_c} \right] = \frac{2}{\Delta} \int \int dk_x dk_z \sum_{i=1}^{2N} \frac{Q_{2n-1}(E_i)}{E_i} \quad (37)$$

IV. TWO AND THREE DIMENSIONS: SPIN-WAVE SPECTRUM AND MAGNETIZATION

Consider just one single xz plane. The above matrix is reduced to two coupled equations

$$\begin{aligned} (E + A_n)g_{n,n'} + B_n f_{n,n'} &= 2 \langle S_n^z \rangle \delta(n, n') \\ -B_n g_{n,n'} + (E - A_n)f_{n,n'} &= 0 \end{aligned} \quad (38)$$

where A_n is given by (32) but without J_{\perp} term for the 2D case considered here. Coefficients B_n and C_n are given by (33) and (34) with $C_n = 0$. The poles of the GF are the eigenvalues of the SW spectrum which are given by the secular equation

$$\begin{aligned} (E + A_n)(E - A_n) + B_n^2 &= 0 \\ [E + A_n][E - A_n] + B_n^2 &= 0 \\ E^2 - A_n^2 + B_n^2 &= 0 \\ E &= \pm \sqrt{(A_n + B_n)(A_n - B_n)} \end{aligned} \quad (39)$$

where \pm indicate the left and right SW precessions. Several remarks are in order:

(i) if $\theta = 0$, we have $B_n = 0$ and the last three terms of A_n are zero. We recover then the ferromagnetic SW dispersion relation

$$E = 2ZJ_{\parallel} \langle S_n^z \rangle (1 - \gamma) \quad (40)$$

where $Z = 4$ is the coordination number of the square lattice (taking $d_n = 0$),

(ii) if $\theta = \pi$, we have $A_n = 8J_{\parallel} \langle S_n^z \rangle$, $B_n = -8J_{\parallel} \langle S_n^z \rangle > \gamma$. We recover then the antiferromagnetic SW dispersion relation

$$E = 2ZJ_{\parallel} \langle S_n^z \rangle \sqrt{1 - \gamma^2} \quad (41)$$

(iii) in the presence of a DM interaction, we have $0 < \cos \theta < 1$ ($0 < \theta < \pi/2$). If $d_n = 0$, the quantity in the square root of Eq. (39) is always ≥ 0 for any θ . It is zero at $\gamma = 1$. The SW spectrum is therefore stable at the long-wavelength limit. The anisotropy d_n gives a gap at $\gamma = 1$.

As said earlier, the necessity to include an anisotropy has a double purpose: it permits a gap and stabilizes a long-range ordering at finite T in 2D systems.

Figure 3 shows the SW spectrum calculated from Eq. (39) for $\theta = 30$ degrees ($\pi/6$ radian) and 80 degrees (1.396 radian). The spectrum is symmetric for positive and negative wave vectors and for left and right precessions. Note that for small θ (i. e. small D) E is proportional to k^2 at low k (cf. Fig. 3a), as in ferromagnets. However, as θ increases, we observe that E becomes linear in k as seen in Fig. 3b. This is similar to antiferromagnets. The change of behavior is progressive with increasing θ , we do not observe a sudden transition from k^2 to k behavior. This feature is also observed in three dimensions (3D) and in thin films as seen below.

It is noted that, thanks to the existence of the anisotropy d , we avoid the logarithmic divergence at $k = 0$ so that we can observe a long-range ordering at finite T in 2D. We show in Fig. 4 the magnetization M ($\equiv \langle S^z \rangle$) calculated by Eq. (35) for one layer using $d = 0.001$. It is interesting to observe that M depends strongly on θ : at high T , larger θ yields stronger M . However, at $T = 0$ the spin length is smaller for larger θ due to the so-called spin contraction [36] calculated by

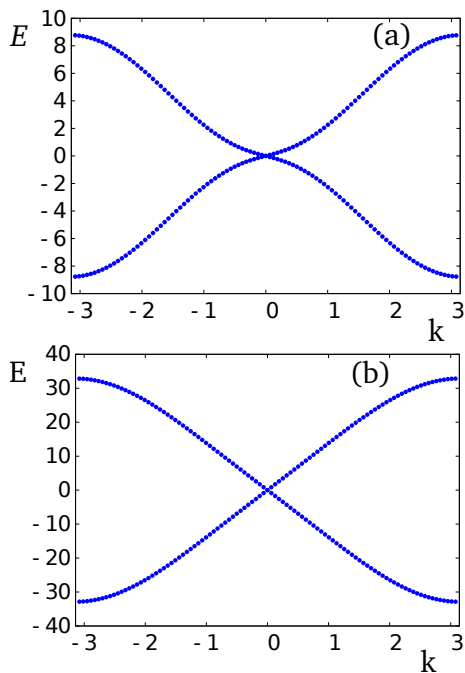


FIG. 3. Spin-wave spectrum $E(k)$ versus $k \equiv k_x = k_z$ for (a) $\theta = 0.524$ radian and (b) $\theta = 1.393$ in two dimensions at $T = 0.1$. Positive and negative branches correspond to right and left precessions. A small $d (= 0.001)$ has been used to stabilized the ordering at finite T in 2D. See text for comments.

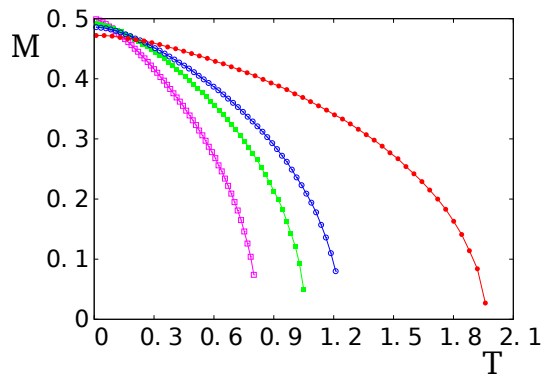


FIG. 4. Magnetizations M versus temperature T for a monolayer (2D) $\theta = 0.175$ (radian), $\theta = 0.524$, $\theta = 0.698$, $\theta = 1.047$ (void magenta squares, green filled squares, blue void circles and filled red circles, respectively). A small $d (= 0.001)$ has been used to stabilized the ordering at finite T in 2D. See text for comments.

Eq. (36). As a consequence there is a cross-over of magnetizations with different θ at low T as shown in Fig. 4.

Let us study the 3D case. The crystal is periodic in three directions. We can use the Fourier transformation in the y direction, namely $g_{n\pm 1} = g_n e^{\pm ik_y a}$ and $f_{n\pm 1} = f_n e^{\pm ik_y a}$. The matrix (30) is reduced to two coupled

equations of g and f functions, omitting index n ,

$$\begin{aligned} (E + A')g + Bf &= 2 \langle S^z \rangle \\ -Bg + (E - A')f &= 0 \end{aligned} \quad (42)$$

where

$$\begin{aligned} A' &= -J_{\parallel} [8 \langle S^z \rangle \cos \theta (1 + d) \\ &\quad - 4 \langle S^z \rangle \gamma (\cos \theta + 1)] \\ &\quad + 4J_{\perp} \langle S^z \rangle \cos(k_y a) \\ &\quad - 4D \sin \theta \langle S^z \rangle \gamma \\ &\quad + 8D \sin \theta \langle S^z \rangle \end{aligned} \quad (43)$$

$$\begin{aligned} B &= 4J_{\parallel} \langle S^z \rangle \gamma (\cos \theta - 1) \\ &\quad - 4D \sin \theta \langle S^z \rangle \gamma \end{aligned} \quad (44)$$

The spectrum is given by

$$E = \pm \sqrt{(A' + B)(A' - B)} \quad (45)$$

If $\cos \theta = 1$ (ferromagnetic), one has $B = 0$. By regrouping the Fourier transforms in three directions, one obtains the 3D ferromagnetic dispersion relation $E = 2Z \langle S^z \rangle (1 - \gamma^2)$ where $\gamma = [\cos(k_x a) + \cos(k_y a) + \cos(k_z a)]/3$ and $Z = 6$, coordination number of the simple cubic lattice. Unlike the 2D case where the angle is inside the plane so that the antiferromagnetic case can be recovered by setting $\cos \theta = -1$ as seen above, one cannot use the above formula to find the antiferromagnetic case because in the 3D formulation it was supposed a ferromagnetic coupling between planes, namely there is no angle between adjacent planes in the above formulation.

The same consideration as in the 2D case treated above shows that for $d = 0$ the spectrum $E \geq 0$ for positive precession and $E \leq 0$ for negative precession, for any θ . The limit $E = 0$ is at $\gamma = 1$ ($\vec{k} = 0$). Thus there is no instability due to the DM interaction. Using Eq. (45), we have calculated the 3D spectrum. This is shown in Fig. 5 for a small and a large value of θ . As in the 2D case, we observe $E \propto k$ when $k \rightarrow 0$ for large θ . Main properties of the system are dominated by the in-plane DM behavior.

Figure 6a displays the magnetization M versus T for several values of θ . As in the 2D case, when θ is not zero, the spins have a contraction at $T = 0$: a stronger θ yields a stronger contraction. This generates a magnetization cross-over at low T shown in the inset of Fig. 6a. The spin length at $T = 0$ versus θ is displayed in Fig. 6b. Note that the spin contraction in 3D is smaller than that in 2D. This is expected since quantum fluctuations are stronger at lower dimensions.

V. THE CASE OF A THIN FILM: SPIN-WAVE SPECTRUM, LAYER MAGNETIZATIONS

In the 2D and 3D cases shown above, there is no need at $T = 0$ to use a small anisotropy d . However in the case of thin films shown below, due to the lack of neighbors at the surface, the introduction of a DM interaction

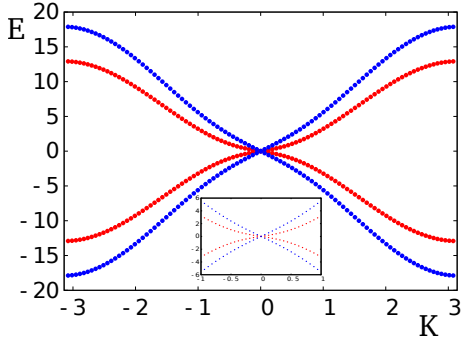


FIG. 5. Spin-wave spectrum $E(k)$ versus $k \equiv k_x = k_z$ for $\theta = \pi/6$ (red circles) and $\theta = \pi/3$ (blue circles) in three dimensions at $T = 0.1$, with $d = 0$. Note the linear- k behavior at low k for the large value of θ (inset). See text for comments.

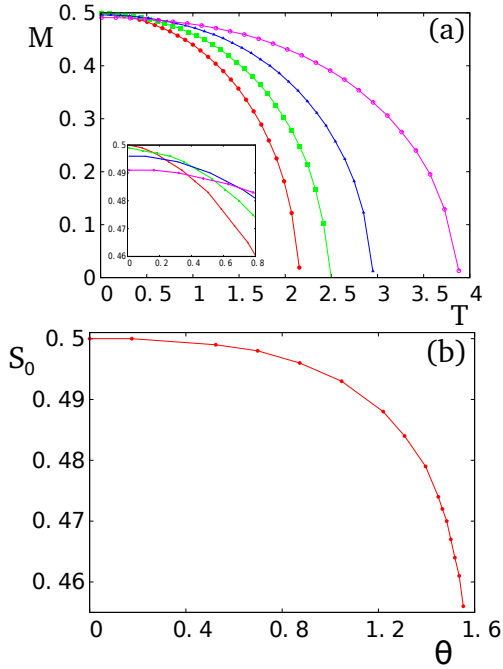


FIG. 6. (a) Magnetization M versus temperature T for a 3D crystal $\theta = 0.175$ (radian), $\theta = 0.524$, $\theta = 0.785$, $\theta = 1.047$ (red circles, green squares, blue triangles and void magenta circles, respectively), with $d = 0$. Inset: Zoom showing the cross-over of magnetizations at low T for different θ , (b) The spin length S_0 at $T = 0$ versus θ . See text for comments.

destabilizes the spectrum at long wave-length $\vec{k} = 0$. Depending on θ , we have to use a value for d_n larger or equal to a "critical value" d_c to avoid imaginary SW energies at $\vec{k} = 0$. The critical value d_c is shown in Fig. 7 for a 4-layer film. Note that at the perpendicular configuration $\theta = \pi/2$, no SW excitation is possible: SW cannot propagate in a perpendicular spin configuration since the wave-vectors cannot be defined.

We show now a SW spectrum at a given thickness N . There are $2N$ energy values half of them are positive and

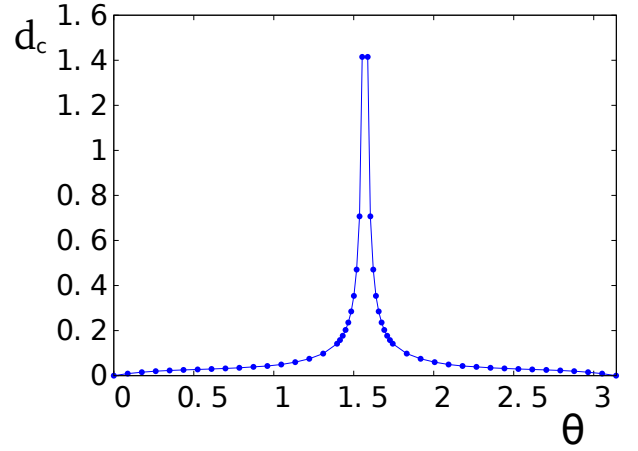


FIG. 7. Value d_c above which the SW energy $E(\vec{k} = 0)$ is real as a function of θ (in radian), for a 4-layer film. Note that no spin-wave excitations are possible near the perpendicular configuration $\theta = \pi/2$. See text for comments.

the other half negative (left and right precessions): E_i ($i = 1, \dots, 2N$). Figure 8 shows the case of a film of 8 layers with $J_{\parallel} = J_{\perp} = 1$ for a weak and a strong value of D (small and large θ). As in the 2D and 2D cases, for strong D , E is proportional to k at small k (cf. Fig. 8b). It is noted that this behavior concerns only the first mode. The upper modes remain in the k^2 behavior.

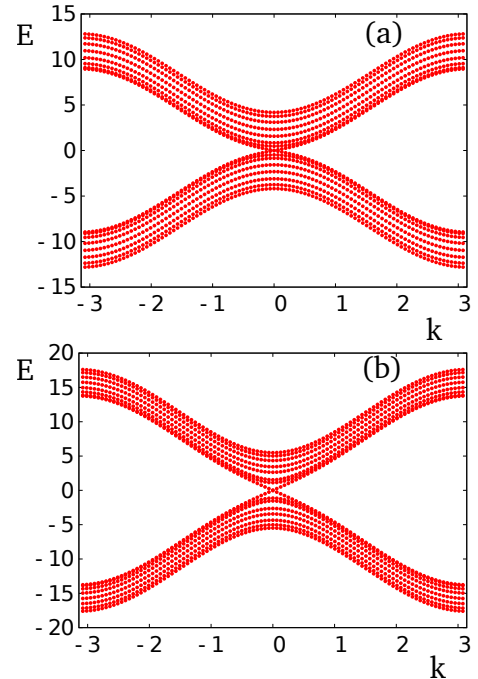


FIG. 8. Spin-wave spectrum $E(k)$ versus $k \equiv k_x = k_z$ for a thin film of 8 layers: (a) $\theta = \pi/6$ (in radian) (b) $\theta = \pi/3$, using $d = d_c$ for each case ($d_c = 0.012$ and 0.021 , respectively). Positive and negative branches correspond to right and left precessions. Note the linear- k behavior at low k for the large θ case. See text for comments.

Figure 9 shows the layer magnetizations of the first four layers in a 8-layer film (the other half is symmetric) for several values of θ . In each case, we see that the surface layer magnetization is smallest. This is a general effect of the lack of neighbors for surface spins even when there is no surface-localized SW as in the present simple-cubic lattice case [36].

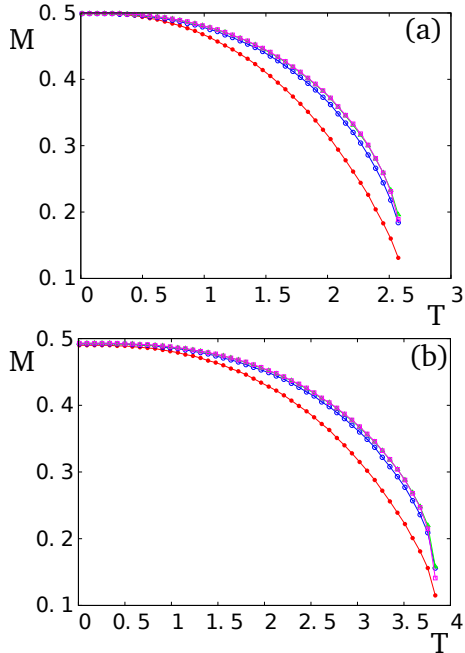


FIG. 9. 8-layer film: layer magnetizations M versus temperature T for (a) $\theta = \pi/6$ (radian), (b) $\theta = \pi/3$, with $d = 0.1$. Red circles, blue void circles, green void triangles and magenta squares correspond respectively to the first, second, third and fourth layer.

The spin length at $T = 0$ for a 8-layer film is shown in Fig. 10 as a function of θ . One observes that the spins are strongly contracted with large θ .

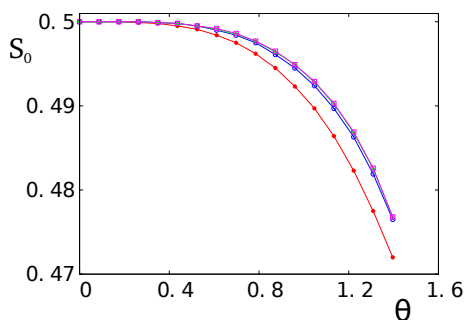


FIG. 10. Spin length S_0 at $T = 0$ of the first 4 layers as a function of θ , for $N = 8$, $d = 0.1$. Red circles, blue void circles, green void triangles and magenta squares correspond respectively to the first, second, third and fourth layer.

Let us touch upon the surface effect in the present model. We know that for the simple cubic lattice, if the

interactions are the same everywhere in the film, then there is no surface localized modes, and this is true with DM interaction (see spectrum in Fig. 8) and without DM interaction (see Ref. 37). In order to create surface modes, we have to take the surface exchange interactions different from the bulk ones. Low-lying branches of surface modes which are "detached" from the bulk spectrum are seen in the SW spectrum shown in Fig. 11a with $J_{||}^s = 0.5$, $J_{\perp}^s = 0.5$. These surface modes strongly affect the surface magnetization as observed in Fig. 11b: the surface magnetization is strongly diminished with increasing T . The role of surface-localized modes on the strong decrease of the surface magnetization as T increases has already been analyzed more than 30 years ago [37].

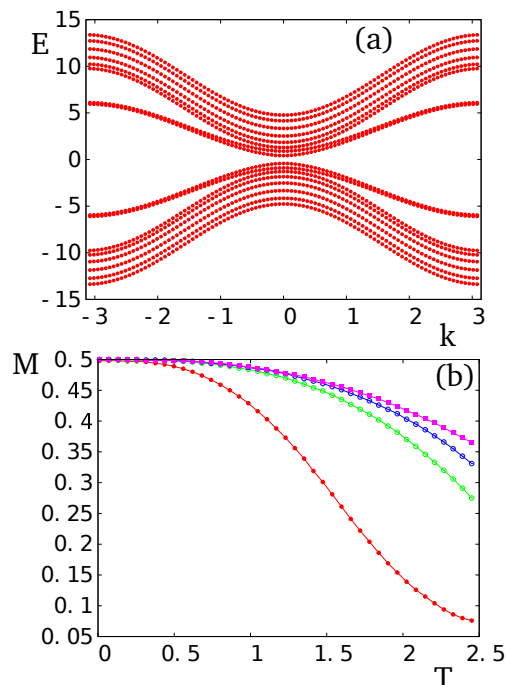


FIG. 11. Surface effect: (a) spin-wave spectrum $E(k)$ versus $k = k_x = k_z$ for a thin film of 8 layers: $\theta = \pi/6$, $d = 0.2$, $J_{||}^s = 0.5$, $J_{\perp}^s = 0.5$, the gap at $k = 0$ is due to d . The surface-mode branches are detached from the bulk spectrum. (b) Layer magnetizations versus T for the first, second, third and fourth layer (red circles, green void circles, blue void circles and magenta filled squares, respectively). See text for comments.

We show now the effect of the film thickness in the present model. The case of thickness $N = 12$ is shown in Fig. 12a with $\theta = \pi/6$ where the layer magnetizations versus T are shown in details. The gap at $k = 0$ due to d is shown in Fig. 12b as a function of the film thickness N for $d = 0.1$ and $\theta = \pi/6$, at $T = 0$. We see that the gap depends not only on d but also on the value of the surface magnetization which is larger for thicker films. The transition temperature T_c versus the thickness N is shown in Fig. 12c where one observes that T_c tends rapidly to the bulk value (3D) which is $\simeq 2.82$ for $d = 0.1$.

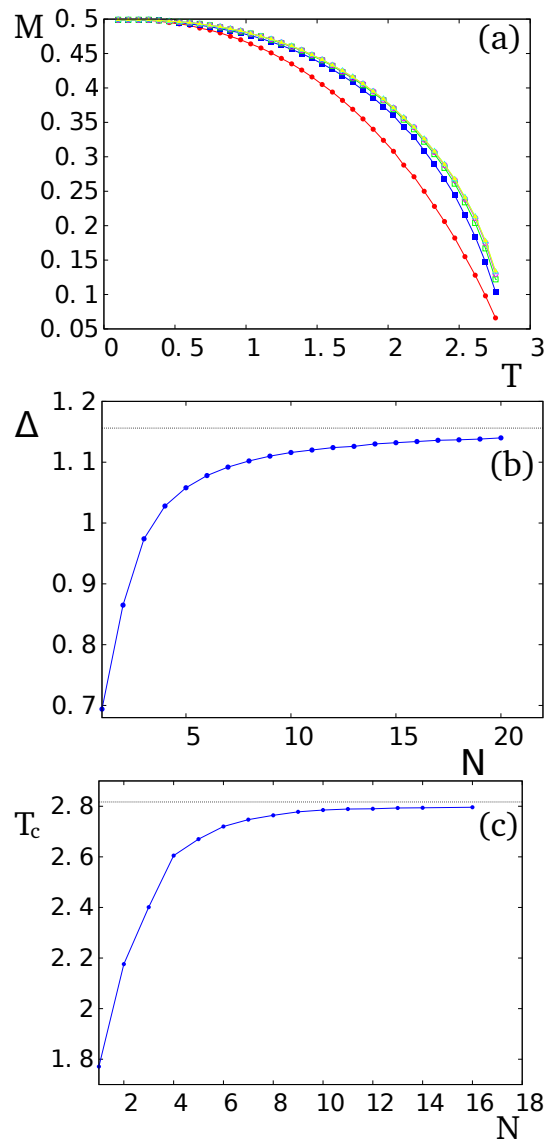


FIG. 12. 12-layer film: (a) Layer magnetizations versus T for $\theta = \pi/6$ and anisotropy $d = 0.1$. Red circles, blue squares, green void squares magenta circles, void turquoise triangles and brown triangles correspond respectively to first, second, third, fourth, fifth and sixth layer, (b) Gap at $k = 0$ as a function of film thickness N for $\theta = \pi/6$, $d = 0.1$, at $T = 0.1$, (c) Critical temperature T_c versus the film thickness N calculated with $\theta = \pi/6$ and $d = 0.1$ using Eq. (37). Note that for infinite thickness (namely 3D), $T_c \simeq 2.8$ for $d = 0.1$.

VI. CONCLUDING REMARKS

By a self-consistent Green's function theory, we obtain the expression of the spin-wave dispersion relation in 2D and 3D as well as in a thin film. Due to the competition between ferromagnetic interaction J and the perpendicular DM interaction D , the GS is non linear with an angle θ which is shown to explicitly depend on the ratio D/J . The spectrum is shown to depend on θ and the layer magnetization is calculated self-consistently as a function of temperature up to the critical temperature T_c .

We have obtained new and interesting results. In particular we have showed that (i) the spin-wave excitation in 2D and 3D crystals is stable at $T = 0$ with the non collinear spin configuration induced by the DM interaction D without the need of an anisotropy, (ii) in the case of thin films, we need a small anisotropy d to stabilize the spin-wave excitations because of the lack of neighbors at the surface, (iii) the spin-wave energy E depends on D , namely on θ : at the long wave-length limit, E is proportional to k^2 for small D but E is linear in k for strong D , in 2D and 3D as well as in a thin film, (iv) quantum fluctuations are inhomogeneous for layer magnetizations near the surface, (v) unlike in some previous works, spin waves in systems with asymmetric DM interactions are found to be symmetric with respect to opposite propagation directions.

ACKNOWLEDGMENTS

This study is a part of a project financed by Narodowe Centrum Nauki (National Science Center of Poland), Grant No. DEC-2013/08/M/ST3/00967. SEH acknowledges a financial support from Agence Universitaire de la Francophonie (AUF).

[1] I. E. Dzyaloshinskii, Sov. Phys. JETP **5**, 1259 (1957).
 [2] T. Moriya, Phys. Rev. **120**, 91 (1960).
 [3] I. A. Sergienko and E. Dagotto, Role of the Dzyaloshinskii-Moriya interaction in multiferroic perovskites, Phys. Rev. B **73**, 094434 (2006).
 [4] Claude Ederer. and Nicola A. Spaldin, Weak ferromagnetism and magnetoelectric coupling in bismuth ferrite, Phys. Rev. B **71**, 060401(R) (2005).
 [5] Maleyev, Phys. Rev. B **73**, 174402 (2006).

[6] Shi-Zeng Lin, Avadh Saxena, and Cristian D. Batista, Phys. Rev. B **91**, 224407 (2015).
 [7] A. N. Bogdanov and D. A. Yablonskii, Sov. Phys. JETP **68**, 101 (1989).
 [8] U.K.Röler, A. N. Bogdanov, and C. Pfleiderer, Nature (London) **442**, 797 (2006).
 [9] S. Mühlbauer, B. Binz, F. Jonietz, C. Pfleiderer, A. Rosch, A. Neubauer, R. Georgii, and P. Böni, Science **323**, 915 (2009).

- [10] X. Z. Yu, Y. Onose, N. Kanazawa, J. H. Park, J. H. Han, Y. Matsui, N. Nagaosa, and Y. Tokura, *Nature (London)* **465**, 901 (2010).
- [11] X. Z. Yu, N. Kanazawa, Y. Onose, K. Kimoto, W. Z. Zhang, S. Ishiwata, Y. Matsui, and Y. Tokura, *Nat. Mater.* **10**, 106 (2011).
- [12] S. Seki, X. Z. Yu, S. Ishiwata, and Y. Tokura, *Science* **336**, 198 (2012).
- [13] T. Adams, A. Chacon, M. Wagner, A. Bauer, G. Brandl, B. Pedersen, H. Berger, P. Lemmens, and C. Pfleiderer, *Phys. Rev. Lett.* **108**, 237204 (2012).
- [14] J. Heurich, J. König, and A. H. MacDonald, *Phys. Rev. B* **68**, 064406 (2003).
- [15] O. Wessely, B. Skubic, and L. Nordstrom, *Phys. Rev. B* **79**, 104433 (2009).
- [16] F. Jonietz, S. Mühlbauer, C. Pfleiderer, A. Neubauer, W. Munzer, A. Bauer, T. Adams, R. Georgii, P. Böni, R. A. Duine, K. Everschor, M. Garst, and A. Risch, *Science* **330**, 1648 (2010).
- [17] M. Heide, G. Bihlmayer, and S. Blgel, Dzyaloshinskii-Moriya interaction accounting for the orientation of magnetic domains in ultrathin films: Fe/W(110), *Phys. Rev. B* **78**, 140403(R) (2008).
- [18] S. Rohart. and A. Thiaville, Skyrmion confinement in ultrathin film nanostructures in the presence of Dzyaloshinskii-Moriya interaction, *Phys. Rev. B* **88**, 184422 (2013).
- [19] A. Fert, V. Cros, and J. Sampaio, *Nat. Nanotechnol.* **8**, 152 (2013).
- [20] A. Yoshimori, *J. Phys. Soc. Jpn* **14**, 807 (1959).
- [21] J. Villain, *Phys. Chem. Solids* **11**, 303 (1959).
- [22] H. Puzskarski and P. E. Wigen, Effect of Dzialoshinsky-Moriya Interactions on Propagation of Spin Waves in Ferromagnets: Dynamical Canting, *Phys. Rev. Lett.* **35**, 1017 (1975).
- [23] Kh. Zakeri, Y. Zhang, J. Prokop, T.-H. Chuang, N. Sakr, W. X. Tang, and J. Kirschner, Asymmetric Spin-Wave Dispersion on Fe(110): Direct Evidence of the Dzyaloshinskii-Moriya Interaction, *Phys. Rev. Lett.* **104**, 137203 (2010)
- [24] Weiwei Wang, Maximilian Albert, Marijan Beg, Marc-Antonio Bisotti, Dmitri Chernyshenko, David Corts-Ortuo, Ian Hawke, and Hans Fangohr, Magnon-Driven Domain-Wall Motion with the Dzyaloshinskii-Moriya Interaction, *Phys. Rev. Lett.* **114**, 087203 (2015).
- [25] A. A. Stashkevich, M. Belmeguenai, Y. Roussigné, S. M. Cherif, M. Kostylev, M. Gabor, D. Lacour, C. Tiusan, and M. Hehn, Experimental study of spin-wave dispersion in Py/Pt film structures in the presence of an interface Dzyaloshinskii-Moriya interaction, *Phys. Rev. B* **91**, 214409 (2015).
- [26] Jung-Hwan Moon, Soo-Man Seo, Kyung-Jin Lee, Kyoung-Whan Kim, Jisu Ryu, Hyun-Woo Lee, R. D. McMichael, and M. D. Stiles, Spin-wave propagation in the presence of interfacial Dzyaloshinskii-Moriya interaction, *Phys. Rev. B* **88**, 184404 (2013).
- [27] V. Thanh Ngo and H. T. Diep, Effects of frustrated surface in Heisenberg thin films, *Phys. Rev. B* **75**, 035412 (2007), Selected for the *Vir. J. Nan. Sci. Tech.* **15**, 126 (2007).
- [28] I. Harada and K. Motizuki, *J. Phys. Soc. Jpn* **32**, 927 (1972).
- [29] H. T. Diep, Low-temperature properties of quantum Heisenberg helimagnets, *Phys. Rev. B* **40**, 741 (1989).
- [30] R. Quartu and H. T. Diep, Phase diagram of body-centered tetragonal Helimagnets, *J. Magn. Magn. Mater.* **182**, 38 (1998).
- [31] V. Thanh Ngo and H. T. Diep, Frustration effects in antiferromagnetic face-centered cubic Heisenberg films, *J. Phys: Condens. Matter.* **19**, 386202 (2007).
- [32] H. T. Diep, Quantum Theory of Helimagnetic Thin Films, *Phys. Rev. B* **91**, 014436 (2015).
- [33] Sahbi El Hog and H. T. Diep, Helimagnetic Thin Films: Surface Reconstruction, Surface Spin-Waves, Magnetization, *J. Magn. and Magn. Mater.* **400**, 276-281 (2016).
- [34] N. D. Mermin and H. Wagner, *Phys. Rev. Lett.* **17**, 1133 (1966).
- [35] H. T. Diep (ed.), *Frustrated Spin Systems*, 2nd edition, World Scientific (2013).
- [36] See for example H. T. Diep, *Theory of Magnetism: Application to Surface Physics*, World Scientific, Singapore (2014).
- [37] Diep-The-Hung, J. C. S. Levy and O. Nagai, Effect of surface spin-waves and surface anisotropy in magnetic thin films at finite temperatures, *Phys. Stat. Solidi (b)* **93**, 351 (1979).